

Thermally activated exchange narrowing of the Gd^{3+} ESR fine structure in a single crystal of $\text{Ce}_{1-x}\text{Gd}_x\text{Fe}_4\text{P}_{12}$ ($x \approx 0.001$) skutterudite

F. A. Garcia,¹ P. A. Venegas,² P. G. Pagliuso,¹ C. Rettori,^{1,3} Z. Fisk,⁴ P. Schlottmann,⁵ and S. B. Oseroff⁶

¹Instituto de Física “Gleb Wataghin,” C.P. 6165, UNICAMP, Campinas-SP 13083-970, Brazil

²UNESP-Universidade Estadual Paulista, Departamento de Física, Faculdade de Ciências, C.P. 473, Bauru-SP 17033-360, Brazil

³Centro de Ciências Naturais e Humanas, Universidade Federal do ABC, Santo Andre-SP 09210-170, Brazil

⁴University of California, Irvine, California 92697, USA

⁵Department of Physics, Florida State University, Tallahassee, Florida 32306, USA

⁶San Diego State University, San Diego, California 92182, USA

(Received 24 March 2011; revised manuscript received 12 July 2011; published 9 September 2011)

We report electron spin resonance (ESR) measurements in the Gd^{3+} doped semiconducting filled skutterudite compound $\text{Ce}_{1-x}\text{Gd}_x\text{Fe}_4\text{P}_{12}$ ($x \approx 0.001$). As the temperature T varies from $T \simeq 150$ K to $T \simeq 165$ K, the Gd^{3+} ESR fine and hyperfine structures coalesce into a broad inhomogeneous single resonance. At $T \simeq 200$ K the line narrows and as T increases further, the resonance becomes homogeneous with a thermal broadening of 1.1(2) Oe/K. These results suggest that the origin of these features may be associated with a subtle interdependence of thermally activated mechanisms that combine: (i) an increase with T of the density of activated conduction carriers across the T -dependent semiconducting pseudogap; (ii) the Gd^{3+} Korringa relaxation process due to an exchange interaction $J_{fd}\mathbf{S}_i\mathbf{s}_i$ between the Gd^{3+} localized magnetic moments and the thermally activated conduction carriers; and (iii) a relatively weak confining potential of the rare earth ions inside the oversized $(\text{Fe}_2\text{P}_3)_4$ cage, which allows the rare earths to become *rattler* Einstein oscillators above $T \approx 148$ K. We argue that the *rattling* of the Gd^{3+} ions, via a motional narrowing mechanism, also contributes to the coalescence of the ESR fine and hyperfine structure.

DOI: [10.1103/PhysRevB.84.125116](https://doi.org/10.1103/PhysRevB.84.125116)

PACS number(s): 71.27.+a, 75.20.Hr, 76.30.-v

I. INTRODUCTION

The filled skutterudite RT_4X_{12} compounds, where R is a rare earth or actinide, T is a transition metal (Fe, Ru, Os), and X is a pnictogen (P, As, Sb) have attracted great attention due to their broad range of physical properties. In particular, they are of interest to those investigating basic mechanisms of strongly correlated electronic systems¹⁻³ and also to those seeking for more efficient thermoelectric materials.^{4,5}

These compounds crystallize in the $\text{LaFe}_4\text{P}_{12}$ structure with space group $Im\bar{3}$ and local point symmetry T_h for the R ions. The R ions are guests in the oversized rigid $(\text{T}_2\text{X}_3)_4$ cages.⁶ The dynamics of the guest R ions is believed to be of great importance in the damping of the thermal conductivity observed in the filled skutterudite compounds.^{7,8} Moreover, they may also play an important role in the appearance of heavy fermion behavior and superconductivity.^{1,9}

Electron spin resonance (ESR) is a sensitive and powerful microscopic tool that provides information about crystal field (CF) effects, site symmetries, valencies of paramagnetic ions, g values, and fine and hyperfine parameters.¹⁰ In a recent work our group¹¹ found ESR to be a sensitive and useful tool to study the dynamics of the R ions in this family of filled skutterudites. The weak confining potential on the R ions at the center of the oversized cage allows them to easily get *off-center* and experience a slightly different local strength and symmetry of the CF which may lead to (i) a distribution of the ESR parameters and (ii) a *rattling* of the R ions that, due to motional narrowing effects,¹² may cause remarkable changes in the observed ESR spectra. In our previous ESR experiments on Yb^{3+} in $\text{Ce}_{1-x}\text{Yb}_x\text{Fe}_4\text{P}_{12}$,¹¹ these two features were observed and the coexistence of two distinct Yb^{3+} sites was confirmed.

Ogita *et al.*,¹³ performing Raman scattering experiments on several metallic skutterudite compounds of the RT_4X_{12} ($T = \text{Fe, Ru, Os}$; $X = \text{P, Sb}$) series, found *resonant* 2nd order phonon modes associated with the vibrations that change the bond length of the R-X stretching mode. However, in semiconducting $\text{CeFe}_4\text{P}_{12}$ the 2nd order phonon modes were found to be *nonresonant*. Based on their results Ogita *et al.*¹³ concluded that there should be a strong coupling between the R-X stretching modes and the conduction electrons (ce). Most reports on the T dependence of the dc resistivity in $\text{CeFe}_4\text{P}_{12}$ present a semiconductorlike behavior.¹⁴ However, the resistivity is strongly sample dependent, and only in some cases it show metallic behavior below $T \approx 200$ K.¹⁵ Nevertheless, for most of the reported samples the conductivity due to thermally activated carriers predominates above $T \approx 200$ K. Thus, for the semiconductor $\text{CeFe}_4\text{P}_{12}$ with a gap of $\simeq 0.15$ eV and an estimated Debye temperature of $\Theta_D \simeq 500$ K,¹⁶ at least a weak coupling of the R-X stretching mode and the ce should be expected. This compound experiences a huge increase in the density of thermally activated conduction carriers at $T \approx 150$ K.¹⁴ Also, evidences for *rattling* of the Yb^{3+} and Ce^{4+} ions were found in ESR¹¹ and extended x-ray absorption fine structure (EXAFS) experiments, respectively. The aim of this work is to learn if the presence of thermally activated conduction carriers and *rattling* of the R ions can be observed by the ESR technique. For that reason we measured the evolution of the Gd^{3+} ESR spectra in $\text{Ce}_{1-x}\text{Gd}_x\text{Fe}_4\text{P}_{12}$ with T . To compare our data with a nonrattling compound, we have also studied the evolution of the Gd^{3+} ESR spectra in $\text{Ca}_{1-x}\text{Gd}_x\text{B}_6$ ($x \approx 0.001$) with T , which is a cubic CsCl type semiconductor with a gap of $\simeq 0.8$ eV and Debye temperature of $\Theta_D \simeq 783$ K.¹⁷

We found that for $\text{Ce}_{1-x}\text{Gd}_x\text{Fe}_4\text{P}_{12}$ the ESR spectra show a different behavior in three T regions. At low T the system behaves as an insulator, at high T as a metal, and in the intermediate region it presents the effects of (a) an exchange interaction $J_{fd}\mathbf{S}_i\mathbf{S}_j$ between Gd^{3+} localized magnetic moments and thermally activated conduction carriers and (b) possible evidence for *rattling* of the R ions.

II. EXPERIMENTAL

Single crystals of $\text{Ce}_{1-x}\text{Gd}_x\text{Fe}_4\text{P}_{12}$ ($x \lesssim 0.001$) were grown in Sn flux as described in Ref. 14. The cubic structure ($Im\bar{3}$) and phase purity were checked by x-ray powder diffraction. Crystals of $\sim 2 \times 2 \times 2 \text{ mm}^3$ of naturally grown crystallographic faces were used in the ESR experiments. Single crystals of $\text{Ca}_{1-x}\text{Gd}_x\text{B}_6$ ($x \lesssim 0.001$) were grown as described in Ref. 18. The cubic structure (space group 221, $Pm\bar{3}m$, CsCl type, and local point symmetry T_d for the R ions) and phase purity were checked by x-ray powder diffraction and the crystals orientation was determined by Laue x-ray diffraction. Most of the ESR experiments were done in $\sim 2 \times 1 \times 0.5 \text{ mm}^3$ single crystals. The ESR spectra were taken in a Bruker X-band (9.48 GHz) spectrometer using appropriated resonators coupled to a T controller of a helium gas flux system for $4.2 \lesssim T \lesssim 300 \text{ K}$. The Gd concentrations were determined from the H and T dependence of the magnetization $M(H, T)$, measured in a Quantum Design superconducting quantum interference device (SQUID) dc magnetometer. In both systems the magnetic susceptibility follows a Curie-Weiss behavior. Also, in both compounds the T dependence of the Gd^{3+} ESR intensity presents a Curie-Weiss-like behavior within the accuracy of the experiments.

III. RESULTS AND DISCUSSION

In both compounds at low T the Gd^{3+} ESR spectra show the full resolved fine structure corresponding to the spin Hamiltonian for the Zeeman and cubic CF interactions, $\mathcal{H} = g\beta HS + b_4 O_4 + b_6 O_6$.¹⁰ The angular and T dependence of the spectra were taken mostly with the applied magnetic field H in the $(1, -1, 0)$ plane. The fitting of the data to the spin Hamiltonian shows that the parameters are, within the experimental accuracy, T independent for the entire studied T range. The measured parameters were $g = 1.986(3)$ and $b_4 = 7(1) \text{ Oe}$ for $\text{Ce}_{1-x}\text{Gd}_x\text{Fe}_4\text{P}_{12}$ and $g = 1.992(3)$ and $b_4 = 13.8(5) \text{ Oe}$ for $\text{Ca}_{1-x}\text{Gd}_x\text{B}_6$, in agreement with previous low- T reports.^{19,20} The accuracy of the data was not enough to estimate the value of b_6 . The g shift measured for Gd^{3+} in $\text{Ce}_{1-x}\text{Gd}_x\text{Fe}_4\text{P}_{12}$ is negative: $\Delta g = 1.986(3) - 1.993 \approx -0.007$. An additional term to the spin Hamiltonian, $J_{fd}\mathbf{S}_i\mathbf{S}_j$, due to a covalent exchange hybridization between the $\text{Gd}^{3+} 4f$ electrons and ce with d character would be responsible for this negative g shift.²¹ For the $\text{Ce}_{1-x}\text{Gd}_x\text{Fe}_4\text{P}_{12}$ crystal, careful measurements of the spectra were taken from $T \simeq 150$ to $T \simeq 200 \text{ K}$ for various directions of H . In this T interval, the fine structure coalesces into a single broad line and its line shape changes from Lorentzian (insulator) to Dysonian (metallic).²² Notice that these features are independent of the field orientation and none of them is observed in $\text{Ca}_{1-x}\text{Gd}_x\text{B}_6$.

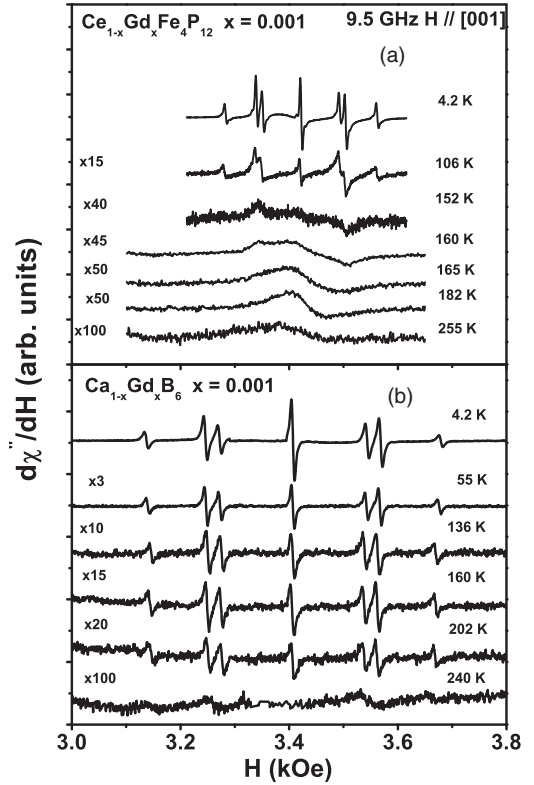


FIG. 1. T dependence of the X-band ESR spectra for $H \parallel [001]$: (a) $\text{Ce}_{1-x}\text{Gd}_x\text{Fe}_4\text{P}_{12}$ and (b) $\text{Ca}_{1-x}\text{Gd}_x\text{B}_6$.

Figures 1–3 display the evolution with T ($4.2 \lesssim T \lesssim 300 \text{ K}$) of the normalized ESR spectra of Gd^{3+} in the $\text{Ce}_{1-x}\text{Gd}_x\text{Fe}_4\text{P}_{12}$ and $\text{Ca}_{1-x}\text{Gd}_x\text{B}_6$ ($x \lesssim 0.001$) crystals for H in the $(1, -1, 0)$ plane along $[001]$, 30° from $[001]$, and $[110]$, respectively. These data show that for $T \gtrsim 150 \text{ K}$ the T dependence of the Gd^{3+} fine structure is quite different in both compounds.

For $\text{Ce}_{1-x}\text{Gd}_x\text{Fe}_4\text{P}_{12}$ the central transition ($\frac{1}{2} \leftrightarrow -\frac{1}{2}$) at 4.2 K and H along $[001]$ is narrow enough to observe the hyperfine satellites lines of the isotopes $^{155,157}\text{Gd}^{3+}$ ($I = 3/2$) (see Fig. 4). The measured hyperfine parameter is $A = 5.5(2) \text{ Oe}$.²³ This hyperfine structure is also observed, although not so clearly, for the other transitions in the spectrum. For the angle where the fine structure collapses (29.6° from $[001]$) and the various transitions overlap, a small misorientation of H by $\lesssim 2^\circ$ away from this direction affects the overall line shape, and the hyperfine structure is then strongly blurred (see Fig. 2). For $\text{Ca}_{1-x}\text{Gd}_x\text{B}_6$ Fig. 4 shows that, due to its higher g value and broader linewidth, the ($\frac{1}{2} \leftrightarrow -\frac{1}{2}$) transition is shifted to lower H and the hyperfine structure is not well resolved. However, the hyperfine parameter can still be estimated to be $A \simeq 7(1) \text{ Oe}$.

Figure 5 presents for both compounds the evolution with T ($4.2 \lesssim T \lesssim 300 \text{ K}$) of the linewidth (ΔH) for the various Gd^{3+} ESR transitions at several H orientations. For $\text{Ce}_{1-x}\text{Gd}_x\text{Fe}_4\text{P}_{12}$ Fig. 5(a) shows the T dependence of ΔH for the ($\frac{1}{2} \leftrightarrow -\frac{1}{2}$) transition and H along $[001]$, $[111]$, and $[110]$ directions and at $\sim 30^\circ$ from $[001]$ in the $(1, -1, 0)$ plane for the collapsed spectrum. It is clear from the data that there are three regions of different T dependence of ΔH : Region I, for $T \lesssim 150 \text{ K}$, where

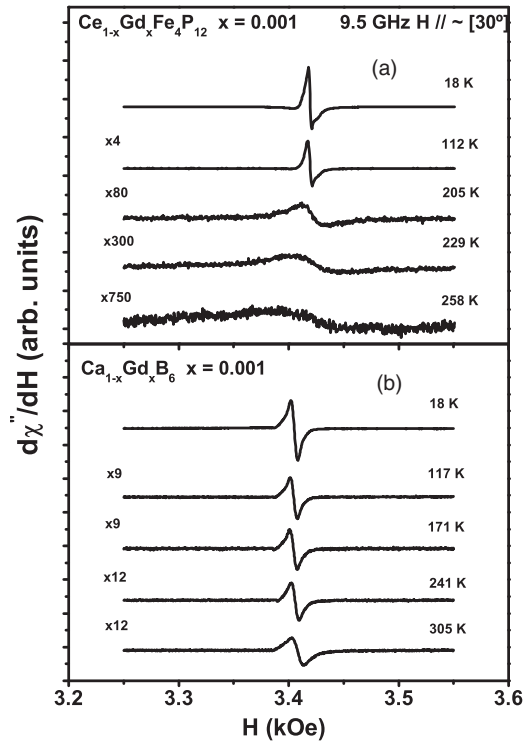


FIG. 2. T dependence of the X-band ESR spectra for H along $\theta \approx 30^\circ$ from $[001]$ in the $(1, -1, 0)$ plane: (a) $\text{Ce}_{1-x}\text{Gd}_x\text{Fe}_4\text{P}_{12}$ and (b) $\text{Ca}_{1-x}\text{Gd}_x\text{B}_6$.

ΔH is nearly T independent and very narrow at $\approx 5(1)$ Oe; Region II, for $165 \lesssim T \lesssim 200$ K, where the full fine structure dramatically coalesces into a broad inhomogeneous

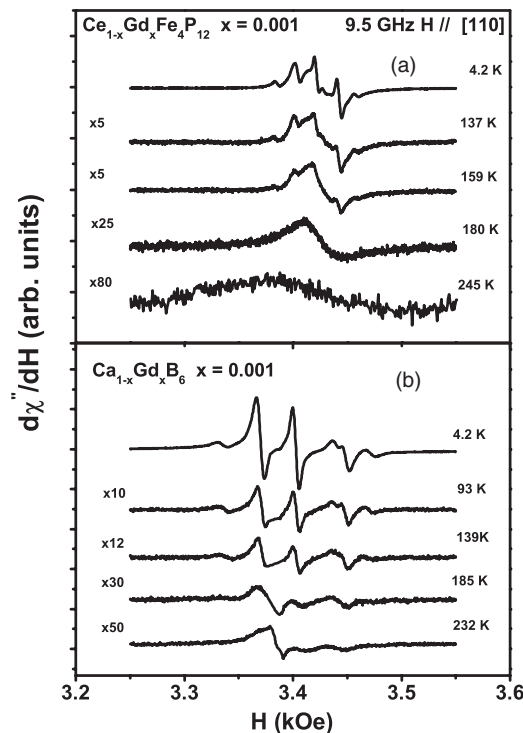


FIG. 3. T dependence of the X-band ESR spectra for $H \parallel [110]$: (a) $\text{Ce}_{1-x}\text{Gd}_x\text{Fe}_4\text{P}_{12}$ and (b) $\text{Ca}_{1-x}\text{Gd}_x\text{B}_6$.

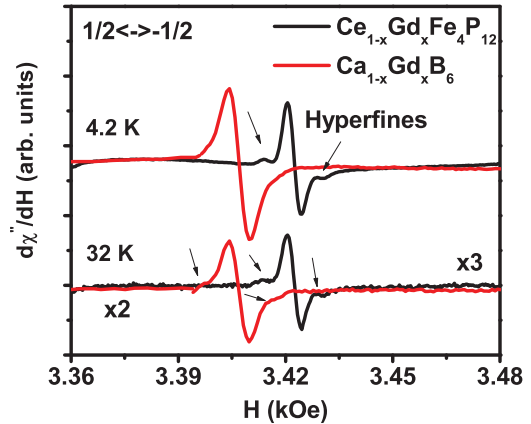


FIG. 4. (Color online) X-band ESR ($\frac{1}{2} \leftrightarrow -\frac{1}{2}$) transition for $H \parallel [001]$. The arrows show the satellite hyperfine structure for both samples of $x = 0.001$.

single resonance with anisotropic ΔH ; and Region III, for $T \gtrsim 200$ K, where ΔH is again isotropic and homogeneous. It corresponds to a single coalesced resonance and has a linear thermal broadening of $\approx 1.1(2)$ Oe/K, reminiscent of a Korringa-like relaxation process via the ce.²⁴

Figures 5(b) and 5(c) show the T dependence of ΔH for the various transitions in $\text{Ce}_{1-x}\text{Gd}_x\text{Fe}_4\text{P}_{12}$ and $\text{Ca}_{1-x}\text{Gd}_x\text{B}_6$ for H along $[001]$ and 30° from $[001]$, respectively. A timid broadening starts to be observed on ΔH for the fine structure components at $T \approx 60$ K for $\text{Ce}_{1-x}\text{Gd}_x\text{Fe}_4\text{P}_{12}$ and at $T \approx 120$ K for $\text{Ca}_{1-x}\text{Gd}_x\text{B}_6$. Presumably this broadening is caused by a phonon spin-lattice relaxation process.²⁵ The fact that such a phonon contribution starts at lower T in $\text{Ce}_{1-x}\text{Gd}_x\text{Fe}_4\text{P}_{12}$ than in $\text{Ca}_{1-x}\text{Gd}_x\text{B}_6$ is consistent with the lower Debye temperature for the former compound. Alternatively, the Gd^{3+} ions produce bound states in the gap, which in the case of CaB_6 are donor states. Carriers bounded at low T in these states can be promoted into the conduction band as T increases and produce a faster relaxation. However, as T increases in Region I a small local distribution of the CF cannot be excluded as the reason for the small broadening of the fine structure lines. The large voided space and concomitant increase of the carrier density as T increases may thermally activate slow motions of the Gd^{3+} ions inside the oversized $(\text{Fe}_2\text{P}_3)_4$ cage which could slightly alter, in an inhomogeneous way, the local CF at the Gd^{3+} site.

As already mentioned, for $\text{Ce}_{1-x}\text{Gd}_x\text{Fe}_4\text{P}_{12}$ above $T \approx 160$ K a dramatic broadening mechanism drives the whole Gd^{3+} resolved ESR fine structure in Region I to coalesce into the broad inhomogeneous and unresolved anisotropic spectrum of Region II [see Fig. 5(a)]. This striking result occurs at about the same T where (i) the density of thermally activated mobile carriers increases by several orders of magnitude [see Fig. 5(d)], (ii) the rattling of the filler R atom is confirmed by EXAFS experiments,¹⁶ (iii) the existence of a T dependent semiconducting pseudogap is observed for $T \lesssim 300$ K in ultraviolet and x-ray photoemission spectroscopies (UPS, XPS),²⁶ and (iv) where the change from Lorentzian (insulator) to Dysonian (metallic) ESR line shape is observed [see Figs. 1(a), 2(a), and 6]. Note that none of these features are present in $\text{Ca}_{1-x}\text{Gd}_x\text{B}_6$. The solid lines in Regions II and III of Fig. 5(a) are the calculated $\Delta H(T)$ for the coalescing

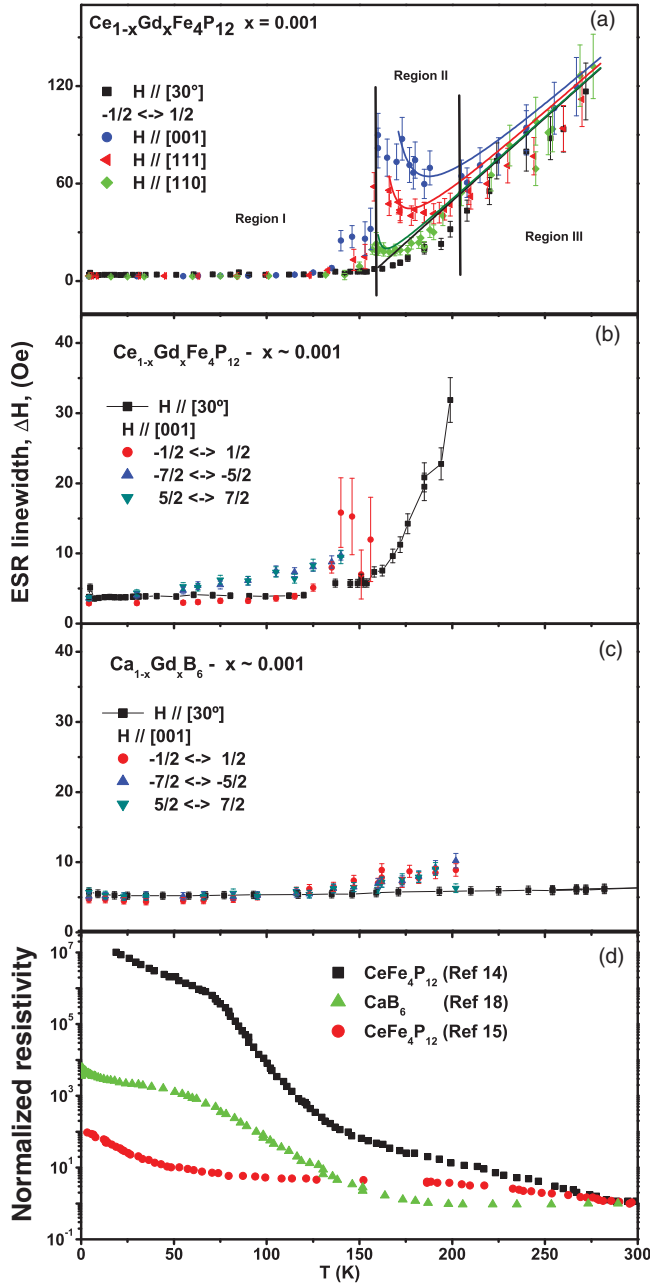


FIG. 5. (Color online) T evolution ($4.2 \lesssim T \lesssim 300$ K) of the Gd^{3+} ESR linewidth ΔH for both compounds and various transitions at several H orientations. Notice that in Fig. 5(a) the behavior of $\Delta H(T)$ clearly characterizes three different regions (I–III). The solid lines in Regions II and III correspond to the calculated $\Delta H(T)$ for the coalesced ESR spectra using the Plefka-Barnes²⁷ exchange narrowing mechanism (see text). Figure 5(d) presents the general T dependence reported for the resistivity in these compounds. The resistivity of our crystals is similar to that of Ref. 14.

ESR spectra using the Plefka-Barnes²⁷ exchange ($J_{fd}\mathbf{S}\cdot\mathbf{s}$) narrowing theory of the fine structure. In the calculation we used a Korringa relaxation of $1.1(2)$ Oe/K that is “switched-on” at $157(2)$ K, a fourth-order CF parameter $b_4 = 7(1)$ Oe, and a residual linewidth $\Delta H(T = 0) = 5(1)$ Oe.

Figure 6 presents the T dependence of the hyperfine structure for the ($\frac{1}{2} \leftrightarrow -\frac{1}{2}$) transition. The data show that the

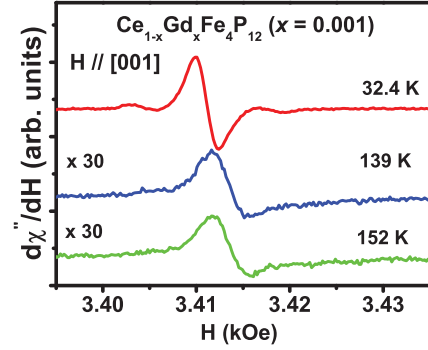


FIG. 6. (Color online) T dependence of the hyperfine structure for the ($\frac{1}{2} \leftrightarrow -\frac{1}{2}$) transition. Notice that the apparent difference in the field for resonance between the low- and high- T spectra is mainly due to the change from Lorentzian to Dysonian, and also to a small change in the frequency of the microwave cavity due to the temperature ($\lesssim 0.05\%$).

coalescence of the hyperfine structure is already observed at $T \approx 150$ K, i.e., at ≈ 15 K below the coalescence of the fine structure at $T \approx 165$ K. This is expected since the exchange interaction would act first on the hyperfine structure due to its much smaller spectral splitting.

Figure 7 shows the angular dependence of ΔH at different T corresponding to Regions II and III. Following the analysis of Urban *et al.*²⁸ for the exchange narrowing of the Gd^{3+} ESR fine structure, the anisotropy of ΔH in Region II can be fitted to the general expression for the intermediate coupling regime:

$$\Delta H = A(T) + B(T)p^2(\theta), \quad (1)$$

where

$$p^2(\theta) = 1 - 5[\sin^2(\theta) + (3/4)\sin^4(\theta)]. \quad (2)$$

Figure 5(a) shows that there is narrowing of ΔH for T approaching 200 K and that the anisotropy decreases, i.e., $B \rightarrow 0$ as $T \rightarrow 200$ K. For $T \gtrsim 200$ K, ΔH becomes isotropic (see Fig. 7) and increases linearly at a rate of $1.1(2)$ Oe/K [see Fig. 5(a)]. This linear increase is an evidence for the presence of a Korringa relaxation process, i.e., the Gd^{3+} ions relax to the lattice via an exchange interaction $J_{fd}\mathbf{S}\cdot\mathbf{s}$ between the

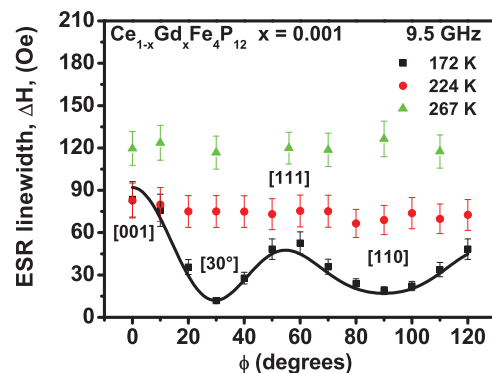


FIG. 7. (Color online) Angular dependence of the ΔH for the Gd^{3+} ESR for temperatures in the Regions II and III of Fig. 5(a). The solid line corresponds to the fitting of the data to Eq. (1) for $A(172 \text{ K}) = 10(3)$ Oe and $B(172 \text{ K}) = 80(10)$ Oe.

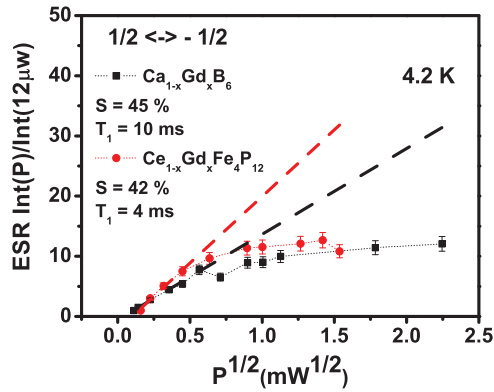


FIG. 8. (Color online) Dependence of the Gd^{3+} ESR intensity at low T on the microwave power for both materials.

Gd^{3+} localized magnetic moment and the thermally activated conduction carriers.²⁴

A g shift of $\Delta g = -0.007$ has been measured for the entire range of T studied for $\text{Ce}_{1-x}\text{Gd}_x\text{Fe}_4\text{P}_{12}$. This is surprising because in Region I there are no conduction carriers that could be polarized. However, the host is a Kondo insulator with a finite Van Vleck susceptibility due to the crystalline field splitting of the Ce ions. This Van Vleck susceptibility is larger than the susceptibility of the thermally excited electrons in Regions II and III and provides the polarization to produce the g shift. This effect is of course not present in the $\text{Ca}_{1-x}\text{Gd}_x\text{B}_6$ sample, since CaB_6 has no significant susceptibility. There is a second unusual issue with the g shift. In a simple metallic host Gd^{3+} ions are expected to have a ferromagnetic Heisenberg exchange. However, the g shift is negative, indicative of a hybridization mechanism. The overlap of the Gd $4f$ electrons with the hybridized Ce $4f$ band forming the valence and conduction bands of the Kondo insulator could give rise to an antiferromagnetic exchange.

It is interesting to note that in Gd^{3+} doped simple metals the Korringa relaxation $d(\Delta H)/dT$ would be related to the g shift Δg by²⁹

$$d(\Delta H)/dT = (\pi k/g\mu_B)(\Delta g)^2. \quad (3)$$

Using our experimental value of $1.1(2)$ Oe/K for $d(\Delta H)/dT$ and 2.34×10^4 Oe/K for $\pi k/g\mu_B$, we estimate a corresponding Δg of $\approx |0.007|$. These results and Eq. (3) suggest that (i) in Region I, where there is no Korringa relaxation, the exchange coupling due to covalent hybridization gives rise to just polarization effects, $J_{fd}(\mathbf{q} = 0)$;³⁰ (ii) the trigger of the Korringa mechanism in Regions II and III is due to the presence of mobile activated conduction carriers at the Fermi level, which are responsible for the momentum transfer between the conduction carriers and the localized magnetic moment via the exchange coupling $J_{fd}(\mathbf{q} \neq 0)$,^{29,30} and (iii) in the metallic Regions II and III, there is no \mathbf{q} dependence of the exchange interaction, i.e., $J_{fd}(\mathbf{q} = 0) \equiv \langle J_{fd}^2(\mathbf{q}) \rangle_{E_F}^{1/2}$.^{29,30}

For $T \lesssim 10$ K Fig. 8 shows that, due to the long spin-lattice relaxation time T_1 in these materials, the Gd^{3+} ($\frac{1}{2} \leftrightarrow -\frac{1}{2}$) transition saturates as a function of the microwave power.³¹ From $\Delta H = (\gamma T_2)^{-1}$ the spin-spin relaxation time can be estimated to be $T_2 \simeq 0.1 \mu\text{s}$ in both compounds. From the

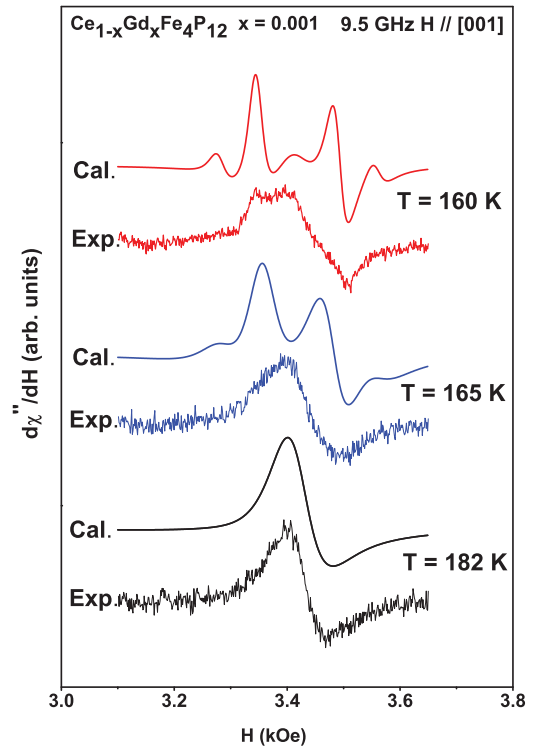


FIG. 9. (Color online) Experimental and calculated²⁷ Gd^{3+} ESR spectra in $\text{Ce}_{1-x}\text{Gd}_x\text{Fe}_4\text{P}_{12}$ for $x = 0.001$ at the transition from Region I to Region II. The parameters used to calculate the theoretical spectra were the same as those used for the calculation of $\Delta H(T)$ in Fig. 5(a).

saturation factor, $S = [1 + (1/4)H_1^2\gamma^2T_1T_2]^{-1}$ and microwave power $P = (1/4)H_1^2$, we estimate the spin-lattice relaxation time to be $T_1 \simeq 10$ ms and $T_1 \simeq 4$ ms for $\text{Ce}_{1-x}\text{Gd}_x\text{Fe}_4\text{P}_{12}$ and $\text{Ca}_{1-x}\text{Gd}_x\text{B}_6$, respectively. Notice that a Korringa relaxation is absent in Region I where the compound behaves as an insulator. Moreover, from ΔH at $T \simeq 300$ K in Fig. 5(a) we estimate $T_1 \simeq 0.002 \mu\text{s}$ which is much shorter than the low T value of T_2 . Therefore, at high T , $T_2 \simeq T_1$ and, as far as ESR is concerned, this is another evidence that $\text{Ce}_{1-x}\text{Gd}_x\text{Fe}_4\text{P}_{12}$ behaves as a regular metal in Regions II and III.

Finally, according to the Raman results and conclusions about the *rattling* modes in metallic skutterudites,¹³ it is plausible that the huge increase in the metallic character of $\text{CeFe}_4\text{P}_{12}$ activates the R-X stretching mode and triggers the *rattling* of the R ions inside the oversized $(\text{Fe}_2\text{P}_3)_4$ cage. Hence, via a motional narrowing mechanism¹² the *rattling* of the Gd^{3+} ions could also contribute to the dramatic change of the ESR spectra observed at the transition from Region I to Region II. Actually Fig. 9 shows that the exchange narrowing mechanism alone cannot reproduce the observed experimental single coalesced resonance at the transition between these two regions. Thus, a motional narrowing of the Gd^{3+} fine structure, due to *rattling* of the R ions, cannot be disregarded, and it probably contributes to the experimental observed spectra. It should be mentioned that such a striking behavior is not expected in $\text{Ca}_{1-x}\text{Gd}_x\text{B}_6$ due to the much larger semiconducting gap of ≈ 0.8 eV and the tighter cages for the CaB_6 compound.

IV. CONCLUSIONS

In this work we have presented experimental data that show the following striking features for the T dependence of the Gd^{3+} ESR spectra in $\text{Ce}_{1-x}\text{Gd}_x\text{Fe}_4\text{P}_{12}$: (a) there is the coalescence of the hyperfine and fine structures at $T \simeq 150$ and $T \simeq 165$ K, respectively; (b) at about these temperatures the ESR line shape changes from Lorentzian (insulating media) to Dysonian (metallic media); and (c) the T dependence of the ESR ΔH changes from a narrow nearly T independent linewidth for each fine structure in Region I to a single inhomogeneous broad resonance with anisotropic ΔH in Region II and then, in Region III, to a homogeneous linewidth with a broadening which is linear in T , resembling the Korringa-like relaxation process in a metallic host.²⁴ Point (b) indicates that, at our microwave frequency and between $T \simeq 150$ and $T \simeq 165$ K, there is also a clear and strong change in the ac conductivity of the material. We associate this change to a *smooth crossover* from insulator to metal which was only possible to be detected due to the high sensitivity that the ESR line shape has in a metallic media.

Our ESR observations in $\text{Ce}_{1-x}\text{Gd}_x\text{Fe}_4\text{P}_{12}$, along with those of Raman, EXAFS, UPS, and XPS for $\text{CeFe}_4\text{P}_{12}$, suggest

that this *smooth insulator-metal* crossover may be responsible for the coalescence and narrowing of the hyperfine and fine structures and also for the activation of the R-X stretching mode that probably triggers the *rattling* of the Gd^{3+} ions in the oversized $(\text{Fe}_2\text{P}_3)_4$ cage. Via a motional narrowing mechanism the Gd^{3+} *rattling* may also contribute to the dramatic change of the ESR spectra at the transition from Region I to Region II.^{11,12}

We believe that our ESR study gives further clues and insights for the subtle interplay between the local vibration modes (Einstein oscillators) of the R ions and the ce in the filled skutterudite compounds. In particular, our work supports the idea that some metallic character is always needed to set up the necessary conditions for the *rattling* of the R ions in these materials.

ACKNOWLEDGMENTS

This work was supported in part by FAPESP, CNPq, CAPES, and NCC from Brazil. P.S. is supported by the US Department of Energy through Grant No. DE-FG02-98ER45707.

-
- ¹T. Goto, Y. Nemoto, K. Sakai, T. Yamaguchi, M. Akatsu, T. Yanagisawa, H. Hazama, K. Onuki, H. Sugawara, and H. Sato, *Phys. Rev. B* **69**, 180511(R) (2004).
- ²E. D. Bauer, A. Slebarski, E. J. Freeman, C. Sirvent, and M. B. Maple, *J. Phys. Condens. Matter* **13**, 4495 (2001).
- ³N. R. Dilley, E. J. Freeman, E. D. Bauer, and M. B. Maple, *Phys. Rev. B* **58**, 6287 (1998).
- ⁴G. J. Snyder and E. S. Toberer, *Nat. Mater.* **7**, 105 (2008).
- ⁵B. C. Sales, D. Mandrus, and R. K. Williams, *Science* **272**, 1325 (1996).
- ⁶W. Jeitschko and D. Braun, *Acta Crystallogr. Sect. A* **33**, 3401 (1977).
- ⁷C. H. Lee, I. Hase, H. Sugawara, H. Yoshizawa, and H. Sato, *J. Phys. Soc. Jpn.* **75**, 123602 (2006).
- ⁸R. P. Hermann, R. Jin, W. Schweika, F. Grandjean, D. Mandrus, B. C. Sales, and G. J. Long, *Phys. Rev. Lett.* **90**, 135505 (2003).
- ⁹T. Yanagisawa, P.-C. Ho, W. M. Yuhasz, M. B. Maple, Y. Yasumoto, H. Watanabe, Y. Nemoto, and T. Goto, *J. Phys. Soc. Jpn.* **77**, 074607 (2008).
- ¹⁰A. Abragam and B. Bleaney, *EPR of Transition Ions* (Clarendon, Oxford, 1970).
- ¹¹F. A. Garcia, D. J. Garcia, M. A. Avila, J. M. Vargas, P. G. Pagliuso, C. Rettori, M. C. G. Passeggi Jr., S. B. Oseroff, P. Schlottmann, B. Alascio, and Z. Fisk, *Phys. Rev. B* **80**, 052401 (2009).
- ¹²P. W. Anderson, *J. Phys. Soc. Jpn.* **9**, 816 (1954).
- ¹³N. Ogita, R. Kojima, T. Haegawa, Y. Takasu, M. Udagawa, T. Kondo, N. Narazu, T. Takabatake, N. Takeda, Y. Ishikawa, H. Sugawara, T. Ikeno, D. Kikuchi, H. Sato, C. Sekine, and I. Shirovani, *J. Phys. Soc. Jpn. Suppl. A* **77**, 251 (2008).
- ¹⁴G. P. Meisner, M. S. Torikachvili, K. N. Yang, M. B. Maple, and R. P. Guertin, *J. Appl. Phys.* **57**, 3073 (1985).
- ¹⁵H. Sato, Y. Abe, H. Okada, T. D. Matsuda, K. Abe, H. Sugawara, and Y. Aoki, *Phys. Rev. B* **62**, 15125 (2000).
- ¹⁶D. Cao, F. Bridges, P. Chesler, S. Bushart, E. D. Bauer, and M. B. Maple, *Phys. Rev. B* **70**, 094109 (2004).
- ¹⁷P. Vonlanthen, E. Felder, L. Degiorgi, H. R. Ott, D. P. Young, A. D. Bianchi, and Z. Fisk, *Phys. Rev. B* **62**, 10076 (2000).
- ¹⁸D. P. Young, D. Hall, M. E. Torelli, J. L. Sarrao, Z. Fisk, J. D. Thompson, H. R. Ott, S. B. Oseroff, R. G. Goodrich, and R. Zysler, *Nature (London)* **397**, 412 (1999).
- ¹⁹R. N. de Mesquita, G. E. Barberis, C. Rettori, M. S. Torikachvili, and M. B. Maple, *Solid State Commun.* **74**, 1047 (1990).
- ²⁰R. R. Urbano, C. Rettori, G. E. Barberis, M. Torelli, A. Bianchi, Z. Fisk, P. G. Pagliuso, A. Malinowski, M. F. Hundley, J. L. Sarrao, and S. B. Oseroff, *Phys. Rev. B* **65**, 180407(R) (2002).
- ²¹G. E. Barberis, D. Davidov, J. P. Donoso, C. Rettori, J. F. Suassuna, and H. D. Dokter, *Phys. Rev. B* **19**, 5495 (1979).
- ²²G. Feher and A. F. Kip, *Phys. Rev.* **98**, 337 (1955); F. J. Dyson, *ibid.* **98**, 349 (1955); G. E. Pake and E. M. Purcell, *ibid.* **74**, 1184 (1948); N. Bloembergen, *J. Appl. Phys.* **23**, 1383 (1952).
- ²³F. A. Garcia, J. G. S. Duque, P. G. Pagliuso, C. Rettori, Z. Fisk, and S. B. Oseroff, *Phys. Status Solidi B* **247**, 647 (2010).
- ²⁴J. Korringa, *Physica* **16**, 601 (1950); H. Hasegawa, *Prog. Theor. Phys. (Kyoto)* **21**, 1093 (1959).
- ²⁵R. Orbach, *Proc. R. Soc. London A* **264**, 458 (1961).
- ²⁶P. A. Rayjada, A. Chainani, M. Matsunami, M. Taguchi, S. Tsuda, T. Yokoya, S. Shin, H. Sugawara, and H. Sato, *J. Phys. Condens. Matter* **22**, 095502 (2010).
- ²⁷T. Plefka, *Phys. Status Solidi B* **51**, K113 (1972); **55**, 129 (1973); S. E. Barnes, *Phys. Rev. B* **9**, 4789 (1974).

²⁸P. Urban, D. Davidov, B. Elschner, T. Plefka, and G. Sperlich, *Phys. Rev. B* **12**, 72 (1975).

²⁹C. Rettori, S. B. Oseroff, D. Rao, P. G. Pagliuso, G. E. Barberis, J. L. Sarrao, Z. Fisk, and M. F. Hundley, *Phys. Rev. B* **55**, 1016 (1997).

³⁰D. Davidov, K. Maki, R. Orbach, C. Rettori, and E. P. Chock, *Solid State Commun.* **12**, 621 (1973).

³¹Charles P. Poole Jr., *Electron Spin Resonance: A Comprehensive Treatise on Experimental Techniques* (Wiley, New York, 1967), p. 707.